

## Seasonal and solar cycle dependences of the correlation between auroral kilometric radiation and the AE index

Atsushi Kumamoto<sup>1\*</sup>, Takayuki Ono<sup>1</sup> and Masahide Iizima<sup>1</sup>

<sup>1</sup>*Department of Geophysics, Graduate School of Science, Tohoku University,  
6-3, Aoba, Aramaki, Aoba, Sendai 980-8578*

*\*Corresponding author. E-mail: kumamoto@stpp1.geophys.tohoku.ac.jp*

(Received December 19, 2004; Accepted April 29, 2005)

**Abstract:** Seasonal and solar cycle dependences of the correlation between auroral kilometric radiation (AKR) and the auroral electrojet (AE) index have been investigated based on the plasma wave data obtained by the Akebono satellite. Under any seasonal and solar activity conditions, a clear correlation has been found between the AKR power flux and the AE index. The properties of the correlation, however, vary depending on season and solar activity. AKR power flux increases as about the 1.2 power of AE index in all seasonal and solar activity conditions. However, even for the same AE index, AKR power flux during solar minimum is 5 dB larger than that during solar maximum. As for the seasonal variations, the AKR power flux in winter is 22 dB larger than that in summer even for the same AE index. The results suggest that long-term variations of AKR depend not only on auroral current variations but also on factors associated with the total energy flux of auroral electrons and the generation process of AKR.

**key words:** auroral kilometric radiation, AE index, seasonal dependence, solar cycle dependence, AKR index

### 1. Introduction

It is widely known that auroral kilometric radiation (AKR) is closely correlated with auroral phenomena. The coincidence of AKR enhancement and discrete aurora appearance was pointed out by Gurnett (1974). Voots *et al.* (1977) showed close correlation between AKR power flux and auroral electrojet (AE) index and proposed to use the AKR power flux as a reliable indicator of geomagnetic disturbances. The idea was developed by studies on “AKR index” (Murata *et al.*, 1997; Kurth *et al.*, 1998; Kurth and Gurnett, 1998). In these studies, the averaged power flux of AKR in frequency range from 50 kHz to 800 kHz was defined as the AKR index and its correlation with K<sub>p</sub> and Dst indices were investigated. Furthermore, the AKR index was also used for identification of the substorm onset in order to discuss the dynamics of plasmoids in the geomagnetic tail (Slavin *et al.*, 1993; Murata *et al.*, 1995).

It has also come to be known that AKR depends not only on geomagnetic conditions but also on seasonal and solar activity conditions. Seasonal variation of AKR is found by statistical studies of long-term plasma wave data obtained by the

Geotail spacecraft and the Akebono (EXOS-D) satellite (Kasaba *et al.*, 1997; Kumamoto and Oya, 1998; Kumamoto *et al.*, 2001). Based on the 13-years of plasma wave data obtained by the Akebono satellite, a solar cycle dependence of AKR was also discovered (Kumamoto *et al.*, 2003a, b). Consistent results were reported based on the statistical analyses of Polar/IMAGE plasma wave datasets (Green *et al.*, 2004). The conditions of the polar ionosphere are likely to be a main control factor of AKR seasonal and solar cycle variations. However, control mechanisms have not been clarified and remain controversial.

In previous studies on AKR index, the seasonal and solar cycle effects on AKR were not taken into account, as pointed out by Green *et al.* (2004). The main purpose of this study is, therefore, to clarify the seasonal and solar cycle effects on the correlation between AKR power flux and AE index by using plasma wave data obtained by the Akebono satellite, and to discuss control factors of AKR seasonal and solar cycle variations.

## 2. Datasets and methods of analysis

AKR power fluxes were derived from high gain and medium gain plasma wave datasets obtained by the plasma waves and sounder (PWS) instrument onboard the Akebono satellite. The instrumentations of the PWS were precisely described by Oya *et al.* (1990). AE indices were provided by World Data Center (WDC) for Geomagnetism, Kyoto. Simultaneous AE indices are available for AKR power flux data in a period from 1990 to 1995. However, it should be noted that the AE index in the period is not final but the provisional one.

In order to investigate seasonal and solar activity dependences of correlations between AKR power flux and AE index, datasets were divided into four groups: Datasets (1) in northern summer during solar maximum, (2) in northern winter during solar maximum, (3) in northern summer during solar minimum, and (4) in northern winter during solar minimum. In this study, summer and winter were defined as three months around the solstice for the northern hemisphere. The period from 1990 to 1991, and the period from 1994 to 1995 were defined as solar maximum and solar minimum, respectively.

The AKR power flux was determined by averaging  $S_{30R_E}$ , normalized power flux at  $30R_E$ , in frequency range from 250 kHz to 800 kHz for 1 min:

$$S_{AKR}(t) = \frac{1}{1 \text{ min}} \int_t^{t+1 \text{ min}} \left[ \frac{1}{550 \text{ kHz}} \int_{250 \text{ kHz}}^{800 \text{ kHz}} S_{30R_E}(f, t) df \right] dt'. \quad (1)$$

Normalized power flux  $S_{30R_E}$  was obtained by

$$S_{30R_E}(f, t) = \left[ \frac{r_{\text{sat}}(t) - r_{f=f_{ce}}(t)}{30R_E} \right]^2 S_{\text{sat}}(f, t), \quad (2)$$

where  $S_{\text{sat}}$ ,  $r_{\text{sat}}$  and  $r_{f=f_{ce}}$  respectively indicate wave power flux at the satellite, geocentric distance of the satellite, and the location at which wave frequency  $f$  equals the local electron cyclotron frequency  $f_{ce}$ . In order to avoid plasma wave data out of the

dynamic range of the PWS in high gain observation mode, only plasma wave data within a power flux range from  $3 \times 10^{-17}$  to  $1 \times 10^{-13} \text{ Wm}^{-2} \text{ Hz}^{-1}$  at the satellite were utilized for the calculations. As for the period from 1990 to 1991, the medium gain plasma wave data, whose dynamic range is from  $3 \times 10^{-15}$  to  $1 \times 10^{-11} \text{ Wm}^{-2} \text{ Hz}^{-1}$ , are also available. However, the amount of the medium gain plasma wave data is much smaller than that of the high gain plasma wave data in the same period. Assuming that AKR is generated near the electron cyclotron frequency at the source and propagates upward, AKR can not be observed below the electron cyclotron frequency at the satellite. In order to determine the AKR power fluxes based on the entire AKR spectrum in the frequency range from 250 to 800 kHz, whose sources are located within a geocentric distance of  $1.85 R_E$ , plasma wave data obtained within a geocentric distance of  $2 R_E$ , were excluded from the analysis. It is also known that AKR mainly occurs in auroral regions in the evening sector (Gurnett, 1974). It should be also considered that AE index is determined by geomagnetic variations observed in the northern polar region. Therefore, only AKR power fluxes obtained in the northern polar area with an invariant latitude range from 70 to 75 degrees and with a magnetic local time (MLT) range from 2200 to 2400 were utilized for the analysis.

### 3. Results

Correlations between the AE index and the normalized AKR power flux,  $S_{\text{AKR}}$ , in the four seasonal and solar activity cases, which are derived from high gain plasma wave datasets, are shown in Figs. 1–4. In each figure, upper panel and lower panel respectively show scatter plot and occurrence time plot of normalized AKR power flux as a function of AE index. Saturation limits of normalized AKR power flux are indicated in the right side of the scatter plot. It should be noted that they depend on the distance between AKR sources and the satellite, which is larger than  $0.15 R_E$  in this analysis because AKR sources in a frequency range above 250 kHz is located within  $1.85 R_E$  and plasma wave data observed within  $2.0 R_E$  are excluded from the analysis. Although the data points are very scattered, we can see the positive correlation between AKR power flux and AE index. In order to investigate seasonal and solar cycle dependence of the correlations, the data points are fitted to  $\log_{10} S_{\text{AKR}} = a \log_{10} AE + b$  by least mean square (LMS) method. The determined parameters are shown in Table 1. Due to scattered property of datasets, correlation coefficients are about 50% or lower in all cases. The fitted lines are also indicated in Figs. 1–4 and summarized in Fig. 6. In summer, AKR power flux increases as about 1.2 power of AE index both during solar maximum and during minimum. However, even for the same AE index, AKR power flux during solar minimum is 5 dB larger than that during solar maximum. In winter, AKR power flux increases as about 1.0 or less power of AE index. However, it should be noted that considerable portion of winter AKR data were excluded from the analysis because they are beyond the saturation level. Due to lack of those data, the slopes of the fitted line can be smaller than it would be if there were no saturation limit. In order to avoid saturation limit effects, plasma wave data obtained by medium gain observation were also utilized for the analysis.

Correlation between the AE index and the normalized AKR power flux in winter

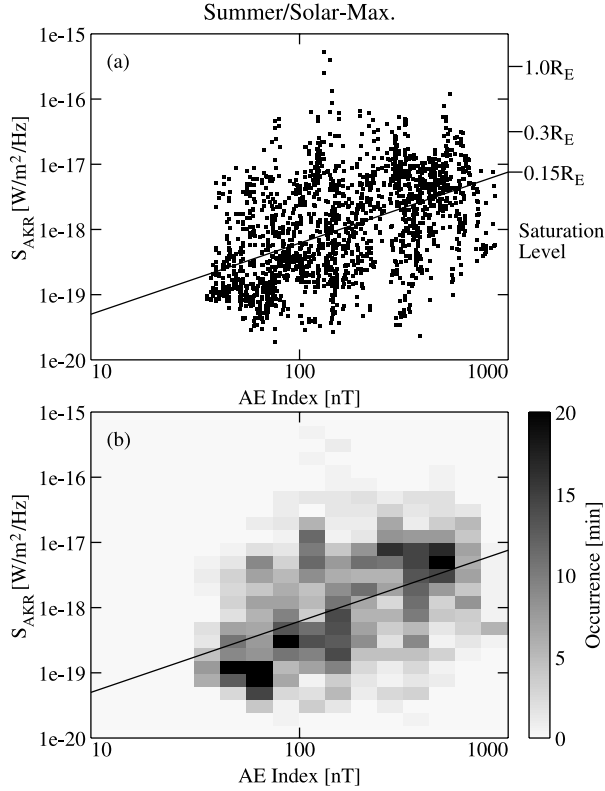


Fig. 1. Scatter plot (a) and occurrence time plot (b) of the normalized AKR power flux as a function of AE index in summer during solar maximum. Normalized AKR power flux and its occurrence time were derived from high gain plasma wave dataset. Fitted line is also indicated by solid line.

during solar maximum, which is derived from medium gain plasma wave dataset obtained in the period from 1990 to 1991, is shown in Fig. 5. Saturation level of medium gain observation is 20 dB larger than those of high gain observation. Therefore, the main portion of winter AKR data can be included in the analysis. Fitted line is shown in Fig. 5 by solid line, and also in Fig. 2 by broken line. In winter during solar maximum, normalized AKR power flux increases about 1.2 power of AE index, which is quite similar to the summer case. During solar maximum, normalized AKR power flux in winter is 22 dB larger than that in summer even for the same AE index.

#### 4. Discussion and conclusions

The results indicated in the previous section clearly suggest that there is a correlation between AKR power flux and AE index in all seasonal and solar activity cases. However the properties of the correlation change depending on season and solar activity. Thus, AKR index proposed in the previous studies should be corrected if it is

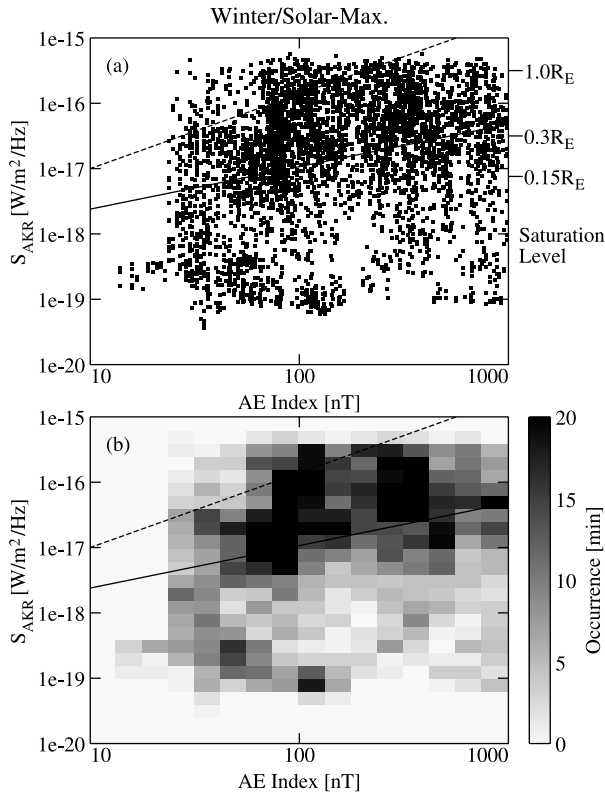


Fig. 2. Scatter plot (a) and occurrence time plot (b) of normalized AKR power flux as a function of AE index in winter during solar maximum. Normalized AKR power flux and its occurrence time were derived from high gain plasma wave dataset. Fitted lines based on high gain and medium gain plasma wave datasets are also indicated by solid line and broken line, respectively.

used under different seasonal and solar activity conditions. Even for the same AE index, there are 5 dB difference between AKR power fluxes during solar maximum and during solar minimum and 22 dB difference between those in the summer and winter polar regions. In the present study, the normalized AKR power flux in winter derived from high gain plasma wave dataset seems to be underestimated due to effects by saturation limit. As for the winter case, the normalized AKR power flux derived from medium gain plasma wave dataset are more reliable than that based on high gain plasma wave dataset.

The AE index were originally defined by Davis and Sugiura (1966) as an indicator of global electrojet activity in the auroral zone. The AE index is derived from geomagnetic variations in the H (horizontal) component observed at selected stations distributed along the auroral zone in the northern hemisphere. The higher and lower envelopes of the H-component perturbation are defined as the AU and AL index. The AE index is determined by  $AE = AU - AL$ . The AE index from 10 to 1000 nT corre-

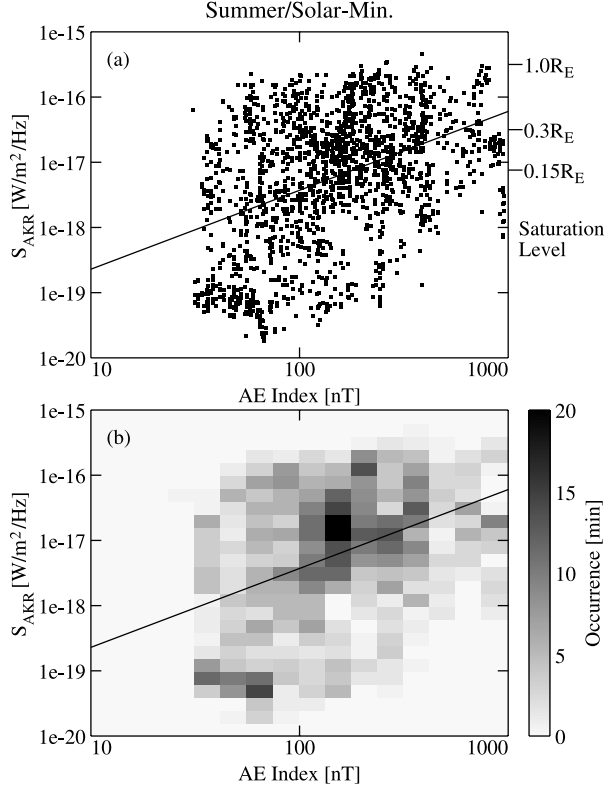


Fig. 3. Same as Fig. 1 but for in summer during solar minimum.

sponds to the current in a range from  $10^4$  to  $10^6$  A in the ionosphere. Based on recent statistical studies on long-term variations of the AE index, it has been reported that the AE index during solar minimum is larger than that during solar maximum (Fres Saba *et al.*, 1997; Ahn and Moon, 2003), which are consistent with the results shown in the present study. On the other hand, based on statistical analysis on annual variation of the AE index, it has been also reported that the AE index increases around the equinox (Lyatsky *et al.*, 2001; Benkevitch *et al.*, 2002). Focusing on the difference between correlations of summer and winter AKR with the AE index, the equinoctial period data were not included into the analyses in the present study. Therefore, the issue on the equinoctial maximum of the AE index and effects on AKR variations are deferred to the future works.

Based on the plasma wave datasets obtained by Imp 6, it has been reported by Voots *et al.* (1977) that correlation between AKR power flux and AE index is given by

$$\log_{10} S_{AKR} = 1.2 \log_{10} AE - 19 \quad (AE > 100 \text{ nT}), \quad (3)$$

$$\log_{10} S_{AKR} = 2 \log_{10} AE - 20.5 \quad (AE < 100 \text{ nT}). \quad (4)$$

These correlations are within fitted lines determined in the present study in summer and winter during solar maximum cases, which is probably because the dataset used by Voots

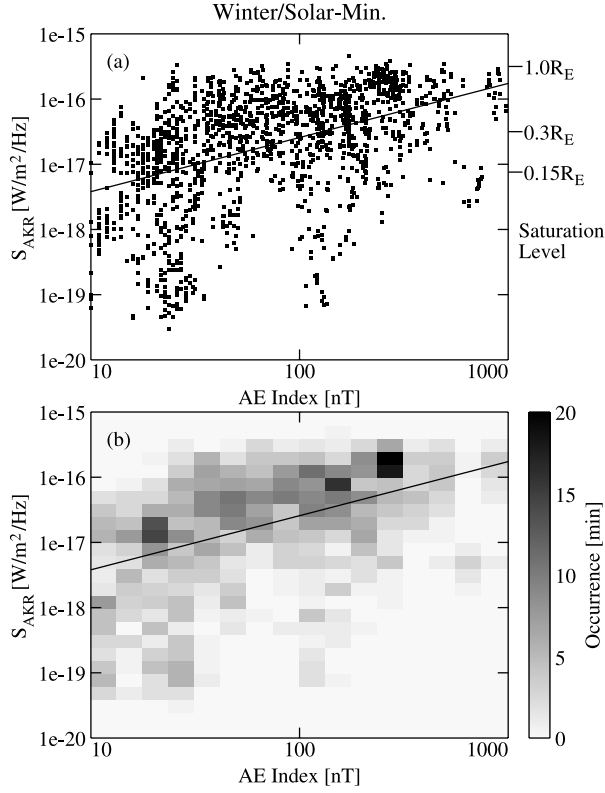


Fig. 4. Same as Fig. 1 but for in winter during solar minimum.

*et al.* (1977) covers autumn and winter during solar maximum. In our results, however, it was difficult to find another slope in AE index range below 100 nT by the LMS method.

Lyons *et al.* (1979) found an empirical relation between the total energy flux of auroral electrons  $E_{\text{tot}}$  and the field aligned potential  $V$ , which is given by

$$E_{\text{tot}} = \alpha \cdot V^2. \quad (5)$$

It was also shown by Fridman and Lamaire (1980) that the parameter  $\alpha$  is given by

$$\alpha = N_{e,M} \frac{e^2}{(2\pi m_e)^{1/2}} \frac{(E_{0\parallel})^{1/2}}{E_{0\perp}}, \quad (6)$$

where  $e$ ,  $m_e$ ,  $N_{e,M}$ ,  $E_{0\parallel}$ , and  $E_{0\perp}$  are charge and mass of electron, number density of hot electrons in the magnetospheric source region such as plasmashheet, and thermal energy parallel and perpendicular to the magnetic field, respectively. Assuming a proportional relation between auroral current and field aligned potential drop as shown by Knight (1973), auroral current is given by

$$I \approx N_e e v_{Te,\parallel} \frac{eV}{T_{e,\perp}} = KV, \quad (7)$$

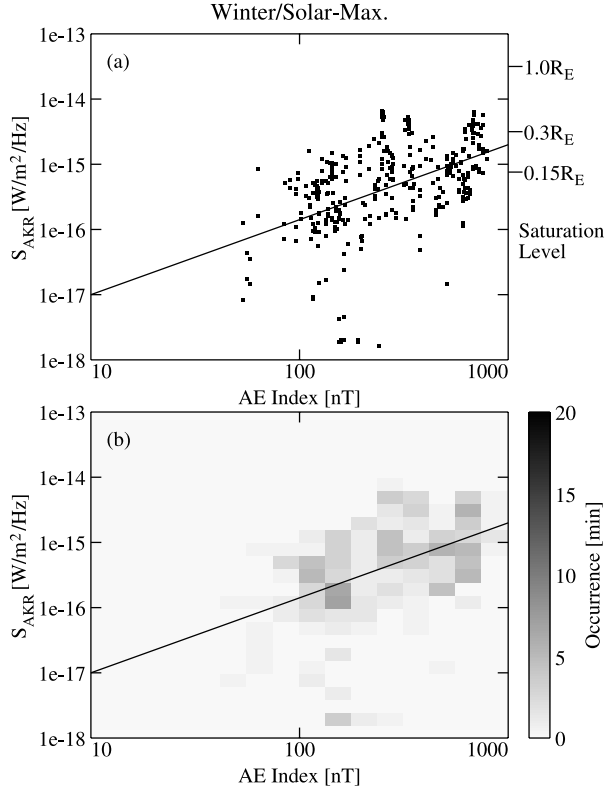


Fig. 5. Same as Fig. 1 but for in winter during solar maximum and from medium gain plasma wave dataset.

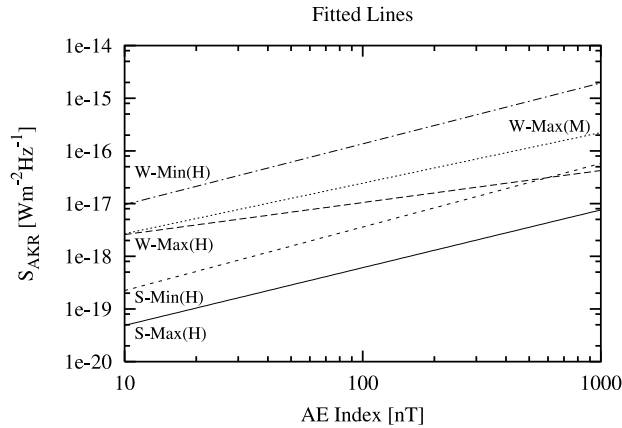


Fig. 6. Seasonal and solar activity dependences of fitted lines for correlations of normalized AKR power flux with AE index. The lines labeled S-Max(H), W-Max(H), S-Min(H), W-Min(H), and W-Max(M) indicated fitted lines for correlations in summer during solar maximum, in winter during solar maximum, in summer during solar minimum, in winter during solar minimum derived from high gain plasma wave datasets, and in winter during solar maximum derived from medium gain plasma wave dataset, respectively.

Table 1. Seasonal and solar activity dependences of least mean square (LMS) fitting parameter  $a$  and  $b$  for correlation of AKR power flux with AE index.  $\sigma_a$ ,  $\sigma_b$ ,  $R$  and  $N$  indicate the standard deviations of  $a$  and  $b$ , correlation coefficient, and data number, respectively.

Dataset	Conditions		$\log_{10} S_{\text{AKR}} = a \log_{10} \text{AE} + b$					
			$\bar{a}$	$\sigma_a$	$\bar{b}$	$\sigma_b$	$R$	$N$
Gain-H	Solar Max.	Summer	1.096	0.044	-20.408	0.097	0.494	1949
		Winter	0.068	0.031	-18.196	0.068	0.277	4789
	Solar Min.	Summer	1.207	0.062	-19.858	0.135	0.412	1884
		Winter	0.960	0.039	-18.532	0.074	0.516	1650
Gain-M	Solar Max.	Winter	1.154	0.118	-18.173	0.286	0.472	337

where  $N_e$ ,  $v_{Te,\parallel}$  and  $T_{e,\perp}$  respectively indicates electron number density, electron thermal velocity parallel to the magnetic field and electron temperature perpendicular to the magnetic field around the field-aligned potential drops in the auroral regions. Using eqs. (5) and (7), AKR power flux  $S_{\text{AKR}}$  is given by

$$S_{\text{AKR}} = \beta E_{\text{tot}} = \beta \frac{\alpha}{K^2} I^\gamma, \quad (8)$$

where  $\gamma=2$ , and  $\beta$  indicates energy conversion efficiency from auroral electrons to AKR. However, as for  $S_{\text{AKR}}$  obtained in this study and in Voots *et al.* (1977),  $\gamma$  is  $\sim 1.2$ . This discrepancy is probably caused not by the change of  $\gamma$  itself but by the changes of other parameter such as  $\beta$  and  $\alpha$ . It is possible that  $\beta$  become small due to some nonlinear saturation mechanisms as the energy flux of auroral electrons increase, as discussed by Voots *et al.* (1977). In addition, it is also inferred that auroral electron precipitation causes loss of hot plasma sources in the magnetosphere, due to which  $\alpha$  can decrease. Ono and Morishima (1994) reported some observational results, in which the apparent  $\gamma$  is less than 2. This is probably because  $\alpha$  decreases as  $I$  increases.

In this study, seasonal and solar cycle dependences of the correlation between AKR power flux and the AE index have been clarified based on the long-term datasets. They are probably attributed to the change of  $\beta/K^2$  caused by seasonal and solar cycle variations in the ionosphere.  $K$  depends on ambient electron density and temperature in an altitude range of several km, where field-aligned potential drops and AKR sources are generated. Even for the same field aligned potentials, or AKR power flux, auroral current varies depending on  $K$ . In summer or during solar maximum,  $S_{\text{AKR}}$  can decrease due to an increase of  $K$ . In this condition, ambient cold plasma in AKR sources becomes dense due to upwelling plasma from the ionosphere. Assuming that AKR is generated via the cyclotron maser instability (CMI) process,  $\beta$  is also inferred to be small in a dense cold plasma (Wu and Lee, 1979; Hewitt *et al.*, 1982).

In this study, AKR power flux clearly depends on the AE index under any seasonal and solar cycle conditions. Therefore, AKR index without seasonal and solar activity correction is sufficiently useful for the purposes such as identification of substorm onsets. However, it should be noted that long-term variations of the AE and AKR indices are

different due to the seasonal and solar activity dependence of  $\beta$  and  $K$ , which is probably caused by variations in the ionosphere. More quantitative investigation of these control factors will be needed for understanding long-term variations of AKR power flux and wide application of the AKR index.

### Acknowledgments

We would like to thank all the staff of the Akebono satellite team. The provisional AE index in the period from 1990 to 1995 was provided by World Data Center (WDC) for Geomagnetism, Kyoto.

The editor thanks Dr. Y. Kasaba and another referee for their help in evaluating this paper.

### References

- Ahn, B.-H. and Moon, G.-H. (2003): Seasonal and universal time variations of the AU, AL and Dst indices. *J. Korean Astron. Soc.*, **36**, S93–S99.
- Benkevitch, L.V., Lyatsky, W.B., Koustov, A.V., Sofko, G.J. and Hamza, A.M. (2002): Substorm onset times as derived from geomagnetic indices. *Geophys. Res. Lett.*, **29** (10), 10.1029/2001GL014386.
- Davis, T.N. and Sugiura, M. (1966): Auroral electrojet activity index AE and its universal time variations. *J. Geophys. Res.*, **71**, 785–801.
- Fres Saba, M.M., Gonzalez, W.D. and Clua de Gonzalez, A.L. (1997): Relationship between the AE, ap and Dst indices near solar minimum (1974) and at solar maximum (1979). *Ann. Geophys.*, **15**, 1265–1270.
- Fridman, M. and Lemaire, J. (1980): Relationship between auroral electrons fluxes and field aligned electric potential differences. *J. Geophys. Res.*, **85**, 664–670.
- Green, J.L., Boardsen, S., Garcia, L., Fung, S.F. and Reinisch, B.W. (2004): Seasonal and solar cycle dynamics of the auroral kilometric radiation source region. *J. Geophys. Res.*, **109**, A05223, doi: 10.1029/2003JA010311.
- Gurnett, D.A. (1974): The earth as a radio source: terrestrial kilometric radiation. *J. Geophys. Res.*, **79**, 4227–4238.
- Hewitt, R.G., Melrose, D.B. and Ronmark, K.G. (1982): The loss-cone driven electron-cyclotron maser. *Aust. J. Phys.*, **35**, 447–471.
- Kasaba, Y., Matsumoto, Hashimoto, K. and Anderson, R.R. (1997): The angular distribution of auroral kilometric radiation observed by the GEOTAIL spacecraft. *Geophys. Res. Lett.*, **24**, 2483–2486.
- Knight, S. (1973): Parallel electric fields. *Planet. Space Sci.*, **21**, 741–750.
- Kumamoto, A. and Oya, H. (1998): Asymmetry of occurrence-frequency and intensity of AKR between summer polar region and winter polar region sources. *Geophys. Res. Lett.*, **25**, 2369–2372.
- Kumamoto, A., Ono, T. and Oya, H. (2001): Seasonal dependence of the vertical distributions of auroral kilometric radiation sources and auroral particle acceleration regions observed by the Akebono satellite. *Adv. Polar Upper Atmos. Res.*, **15**, 32–42.
- Kumamoto, Ono, T., Iizima, M. and Oya, H. (2003a): Seasonal and solar cycle variations of the vertical distribution of the occurrence probability of auroral kilometric radiation sources and of upflowing ion events. *J. Geophys. Res.*, **108** (A1), 1032, doi: 10.1029/2002JA009522.
- Kumamoto, A., Ono, T., Iizima, M. and Oya, H. (2003b): Control factor of solar cycle variation of auroral kilometric radiation. *Adv. Polar Upper Atmos. Res.*, **17**, 48–59.
- Kurth, W.S. and Gurnett, D.A. (1998): Auroral kilometric radiation integrated power flux as proxy for AE. *Adv. Space Res.*, **22**, 73–77.
- Kurth, W.S., Murata, T., Lu, G., Gurnett, D.A. and Matsumoto, H. (1998): Auroral kilometric radiation and the auroral electrojet index for the January 1997 magnetic cloud event. *Geophys. Res. Lett.*, **25**,

- 3027–3030.
- Lyatsky, W., Newell, P.T. and Hamza, A. (2001): Solar illumination as cause of the equinoctial preference for geomagnetic activity. *Geophys. Res. Lett.*, **28**, 2353–2356.
- Lyons, L.R., Evans, D.S. and Lundin, R. (1979): An observed relation between magnetic field aligned electric fields and downward electron energy fluxes in the vicinity of auroral forms. *J. Geophys. Res.*, **84**, 457–461.
- Murata, T., Matsumoto, H., Kojima, H., Fujita, A., Nagai, T., Yamamoto, T. and Anderson, R.R. (1995): Estimation of tail reconnection lines by AKR onsets and plasmoid entries observed with GEOTAIL spacecraft. *Geophys. Res. Lett.*, **22**, 1849–1852.
- Murata, T., Matsumoto, H., Kojima, H. and Iyemori, T. (1997): Correlations of AKR index with  $K_p$  and Dst indices. *Proc. NIPR Symp. Upper Atmos. Phys.*, **10**, 64–68.
- Ono, T. and Morishima, K. (1994): Energy parameters of precipitating auroral electrons obtained by using photometric observations. *Geophys. Res. Lett.*, **21**, 261–264.
- Oya, H., Morioka, A., Kobayashi, K., Iizima, M., Ono, T., Miyaoka, H., Okada, T. and Obara, T. (1990): Plasma wave observation and sounder experiments (PWS) using the Akebono (EXOS-D) satellite-instrumentation and initial results including discovery of the high altitude equatorial plasma turbulence. *J. Geomagn. Geoelectr.*, **42**, 411–442.
- Slavin, J.A., Smith, M.F., Mazur, E.L., Baker, D.N., Hones, E.W., Iyemori, T. and Greenstadt, E.W. (1993): ISEE 3 observations of traveling compression regions in the earth's magnetotail. *J. Geophys. Res.*, **98**, 15425–15446.
- Voots, G.R., Gurnett, D.A. and Akasofu, S.-I. (1977): Auroral kilometric radiation as an indicator of auroral magnetic disturbances. *J. Geophys. Res.*, **82**, 2259–2266.
- Wu, C.S. and Lee, L.C. (1979): A theory of the terrestrial kilometric radiation. *Astrophys. J.*, **230**, 621–626.